

JAM Chem Soc. Author manuscript; available in PIVIC 2014 July 10.

Published in final edited form as:

J Am Chem Soc. 2013 July 10; 135(27): 9968–9971. doi:10.1021/ja400021x.

N,C-capped dipeptides with selectivity for mycobacterial proteasome over human proteasomes: Role of S3 and S1 binding pockets

Gang Lin¹, Tamutenda Chidawanyika¹, Christopher Tsu², Thulasi Warrier¹, Julien Vaubourgeix¹, Christopher Blackburn², Kenneth Gigstad², Michael Sintchak², Lawrence Dick², and Carl Nathan¹

Gang Lin: gal2005@med.cornell.edu; Carl Nathan: cnathan@med.cornell.edu

¹Department of Microbiology and Immunology, Weill Cornell Medical College, 1300 York Avenue, New York, NY 10065, USA

²Millennium Pharmaceuticals Inc., 40 Landsdowne Street, Cambridge, MA 02139, USA

Abstract

We identified N,C-capped dipeptides that are selective for the *Mycobacterium tuberculosis* proteasome over human constitutive and immunoproteasomes. Differences in S3 and S1 binding pockets appeared to account for species-selectivity. The inhibitors are able to penetrate mycobacteria and kill non-replicating *M. tuberculosis* under nitrosative stress.

Unique features of enzymes from different species can provide a structural basis for development of species-selective inhibitors, even when the enzymes are highly conserved. Proteasome 20S core particles are found in all three kingdoms of life, with 14 copies of and 14 copies of subunits forming a barrel-shaped complex of 4 rings, 7 7 7 7. Eukaryotic proteasomes that are widely and constitutively (c-20S) expressed have 7 different copies of and , respectively, but only 3 of the subunits, namely 1, 2, and 5, are enzymatically active. Humans also express an immunoproteasome (i-20S) constitutively in immune cells and inducibly in other cells in response to certain cytokines. ²⁻⁴ In the i-20S, 1, 2, and 5 are replaced by 1i, 2i, and 5i. The replacements result in changes in many aspects of the immune response, indicating the importance of the i-20S in the immune system. ⁵ In contrast, eubacterial proteasomes usually have only 1 and rarely 2 types of and subunits, and all subunits are active. *Mycobacterium tuberculosis* (Mtb) is the only known bacterial pathogen with a proteasome. Mtb genes *prcB* and *prcA* encode and subunits, respectively. ⁶ The Mtb proteasome plays vital roles in defense of the pathogen against nitrosative stress *in vitro*⁷ and in persistence in mice. ^{8,9}

New drugs are needed that can kill the non-replicating populations of Mtb against which few existing drugs are active. ¹⁰ In our initial pursuit of inhibitors that are selective for Mtb proteasomes over human proteasomes, we exploited structural differences ¹¹ in S1 binding pockets and identified peptide boronates whose P1 amino acids conferred modest selectivity (up to 8-fold) for Mtb20S over hu c-20S. ¹¹ We then identified 1,3,4-oxathiazol-2-ones with up to 1300-fold species selectivity. Selectivity appeared to depend on a unique mechanism

Correspondence to: Gang Lin, gal2005@med.cornell.edu; Carl Nathan, cnathan@med.cornell.edu. The authors declare no competing financial interest.

Supporting Information. Reagents, assays, synthesis, Scheme S1, and Figures S1-6. This material is available free of charge via the Internet at http://pubs.acs.org.

involving induction of a conformational change in the Mtb proteasome. ¹² Inhibition of the Mtb proteasome is bactericidal in Mtb that has been rendered non-replicating by sublethal levels of reactive nitrogen intermediates, ^{7,12} an important component of host defense against Mtb. ^{13,14} Instability of oxathiazolones in serum (see below) spurred efforts to find new pharmacophores active on the Mtb proteasome that spare both the human constitutive proteasome and immunoproteasome. ¹⁵ Recently, crystal structures of mouse c-20S and i-20S were solved, and a comparison of the c-20S and i-20S showed that the S1 binding pockets of the 5 and 5i subunits are different enough to design inhibitors that are selective for i-20S over c-20S. ¹⁶ Herein we report a new class of inhibitors that selectively inhibit the Mtb proteasome over human proteasomes by taking advantage of structural differences in both the S1 and S3 binding pockets between the Mtb20S and both human c-20S and i-20S.

A library of 1600 N,C-capped dipeptides was constructed by varying P4 (the N-cap), P3 and P2 (using natural or unnatural amino acids), and P1 (the C-cap). ¹⁷ Kinetic studies indicated that this class of compounds acts as rapid-equilibrium, reversible and competitive inhibitors of human proteasomes. X-ray crystallography of the complex of one such compound (ML16, Fig. S1) with the yeast 20S proteasome confirmed that the C-cap projected into the S1 binding pocket (Fig. 1), the first amino acid residue occupied the S2 pocket and the second amino acid residue the S3 pocket.¹⁷ We screened this library against the Mtb20S open gate mutant. Of the 1600 compounds tested, 65 inhibited purified recombinant Mtb20SOG 80% at 2 µM. For 60 of these, IC₅₀s were determined by monitoring the hydrolysis of suc-LLVY-AMC by Mtb20SOG at 37°C. IC₅₀s were then converted to K_i according to equation $K_i = IC_{50}/(1+[S]/K_M)$ (Table 1). Of these, 6 compounds had >100-, 2 had >500- and 1 had >1000-fold selectivity for Mtb20SOG over human constitutive proteasome 5 subunit, and 13 compounds showed <100 nM potency. The most potent shared several features: P1: 2,4-diF-benzyl as C-cap; P2: 4-F-phenyl; P3: Asn derivatives; and P4: 3-phenylpropanoyl. The most species selective compounds shared a common feature—a fully substituted N-atom on the P3-Asn amide side chain, in contrast to the preference of Hu20S for the secondary amide neopentyl-Asn. Compounds ML2 and ML9 were highly potent with K_i 30 nM and 63 nM, respectively, and highly selective with 121and > 1590-fold species selectivity, respectively.

$$[P] = v_s t + \frac{(v_i - v_s)}{k_{obs}} (1 - e^{(-k_{obs}t)}) \quad (1)$$

$$k_{obs} = k_{on}[I] + k_{off}$$
 (2)

$$\frac{V_i}{V_0} = \frac{1}{1 + [I]/K_i}$$
 (3)

$$K_i = \frac{K_i^{app}}{1 + [S]/K_{ii}}$$
 (4)

To improve upon ML9, we took advantage of prior work demonstrating that the Mtb20S S1 site prefers larger P1 aromatic residues as compared to c-20S. ¹¹ We therefore designed and synthesized (Scheme S1) two analogs of ML9, DPLG-2 and DPLG-4. DPLG-2 incorporates P1-naphthyl, while DPLG-4 contains an isopropyl substitution to test if the S1 binding site can tolerate bulkier substituents at the 4-position of the P1 phenyl ring (Fig. 1). Each maintains the P3-*N*,*N*-diethyl Asn amide for the S3 binding site. DPLG-2 showed 4-fold

increase in potency (K_i 15 nM) against Mtb20SOG compared to ML9; however, DPLG-4 (K_i 770 nM vs Mtb20SOG) showed ~an 18-fold increase in K_i compared to ML9, indicating that the bulky group at the 4-position of the P1 phenyl ring is not well tolerated by the S1 pocket of the Mtb proteasome.

Contrary to the rapid-equilibrium inhibition shown by ML9, ¹⁷ DPLG-2 inhibited Mtb20SOG in a time-dependent manner (Fig. 2A). Mtb20OG (48 nM) was pre-incubated with and fully inactivated by DPLG-2 (2.5 µM) and then diluted into buffer containing substrate and the recovery of activity was recorded for ~ 25 minutes (Fig. S2). The recovery data points were fitted to Eq. (1) to determine the dissociation rate constant $k_{\rm off} = 0.0015 \pm 0.0015$ 0.0001 s^{-1} , which indicated that the half-life of the enzyme-inhibitor complex is 7.7 minutes. To determine the association rate constant, the proteolytic reaction progress curves in the presence of DPLG-2 at various concentrations were recorded and the data points were fitted to equation (1) to determine k_{obs} at each inhibitor concentration (Fig. 2B). Plotting $k_{\rm obs}$ against the inhibitor concentrations and fitting to equation (2) gave apparent $k_{\rm on}$ 5.7 \pm $0.2 \times 10^4 \,\mathrm{M^{-1} s^{-1}}$ (Fig. 2C). The apparent K_i^{app} of DPLG-2 against Mtb20SOG was determined to be 24.2 ± 0.9 nM by plotting V_i/V_0 against inhibitor concentration and fitting to equation (3) (Fig. 2D). This agreed well with the K_i^{app} 26.3 nM calculated from k_{off}/k_{on} . The K_i 15 nM was then calculated from equation (4). DPLG-2 was 4-fold more potent against Mtb20SOG than ML9, with greater species selectivity (4670-fold) (k_i vs human c-20S 70 µM) (Table 2). The underlying reason for the change of mechanism from rapidequilibrium to slow-binding inhibition is under investigation.

Availability of crystal structures allowed us to compare the binding pockets of Mtb20S and eukaryotic proteasomes. As shown in Fig. 3, the S3 binding pocket of the Mtb20S differs significantly from that of yeast 20S, mouse c-20S and mouse i-20S. The P3-neopentyl asparagine residue of ML16 perfectly fits into the S3 site of the mammalian proteasomes (Fig. 3A, C, D) but poorly in the S3 site of the Mtb proteasome (Fig. 3B). Although the S1 binding pockets of the Mtb20S and the c-20S are substantially different, they are similar between the Mtb20S and the i-20S, and both proteasomes were shown to prefer larger aromatic groups at P1 position of the N-acetyl tripeptide-AMC substrates (Fig. S3). 11,17 To test if dipeptides that were selective for the Mtb proteasome over the human constitutive proteasome were comparably poor inhibitors of the human i-20S, we measured IC_{50} 's and converted them to K_i 's as above for selected compounds (Table 2). In agreement with the structural analysis, ML9 and DPLG-2 inhibited human i-20S 5i poorly with K_i 26.3 μ M and 54.7 µM, respectively. However, ML2 showed potent inhibitory activity against i-20S with K_i 0.82 μ M. Given that both ML9 and DPLG-2 have same P3 N_i N-diethylamide moiety, whereas ML2 has a P3 pyrrolidinylamide moiety, which is much less bulky, it indicates that the S3 binding pocket dictates the species selectivity between Mtb20S and both human c-20S and i-20S, and an acyclic, fully substituted Asn side chain is required for selectivity against both the c-20S and the i-20S. The shift to a slow-binding mechanism suggests that binding may stabilize an altered conformation. Consistent with this, the P1naphthyl moiety cannot be docked into the crystallographically determined S1 pocket of the Mtb20S (Fig. S4).

To test if the dipeptides were mycobactericidal toward non-replicating Mtb under nitrosative stress, we incubated Mtb in 0.5 mM NaNO₂ at pH 5.5 in Sauton's medium overnight and then added dipeptides at indicated concentrations for 5 or 11 days (Fig. 4A). ML2, ML9 and DPLG-2 were cidal, with up to $1 \log_{10}$ reduction in colony-forming units after 5 days and up to $2.2 \log_{10}$ of killing after 11 days, at concentrations that were greater than twice their K_i 's. Above 100 nM, there was no significant increase in the extent of killing when the concentrations of the inhibitors were increased to $25 \,\mu$ M. Killing was dependent on dose (Fig. 4A inset), nitrosative stress (Fig. S5A, B) and prcBA (Fig. S5C). The incomplete

extent of killing phenocopied the Mtb *prcBA* knockout over the same time period in non-replicating conditions.^{8,9} That the bacteria were not completely eradicated mirrors the action of many other compounds active on non-replicating Mtb, eg Dlat inhibitor¹⁸ and rifampin (not shown). As discussed in the Supporting Information, treatment with N,C-capped dipeptides did not phenocopy *prcBA* deficiency competely, perhaps because the dipeptides did not inhibit the proteasome completely. In contrast to 1,3,4-oxathiazol-2-ones, DPLG-2 was stable in human plasma over 22 hours (Fig. S6).

Ability to kill Mtb provided strong evidence that the dipeptides entered the bacteria, but this would be difficult to confirm by testing for proteasome inhibition in lysates prepared from dipeptide-treated Mtb, because binding would be reversed when the cells were washed and lysed. To circumvent this problem, we devised a competition assay, in which we took advantage of HT1171, an oxathiazolone that can enter Mtb and inhibit its proteasome irreversibly. 12 We reasoned that if the dipeptides could prevent the inhibition of the Mtb proteasome inside intact mycobacteria by HT1171, this would indicate that the dipeptides had penetrated the mycobacteria and bound to the proteasome active site. Mid-log phase cells of M. bovis strain BCG were incubated with DPLG-2 at indicated concentrations for 4 hours prior to addition of HT1171 (25 µM) for a further 1 hour. Cells were washed extensively to remove unbound inhibitors of both types. The proteasomal activities of the lysates (Fig. 4B) were determined as reported. 12 In the absence of DPLG-2 or in the presence of concentrations of DPLG-2 (1 µM) that were low relative to HT1171 (25 µM), HT1171 inhibited the proteasomes irreversibly, as before. However, 10 µM and 50 µM of DPLG-2 were able to shield the mycobacterial proteasome active sites from HT1171. Thus, DPLG-2 could penetrate mycobacteria and bind to proteasome active sites in situ. Efforts to conduct a similar competition experiment with Me4BodipyFL-Ahx3Leu3VS were not possible, as that probe afforded only 8% inhibition of the Mtb proteasome, in accord with earlier work.¹¹

In summary, we have identified a series of N,C-capped dipeptides that are highly selective for the Mtb proteasome over both human constitutive and human immunoproteasomes and can penetrate Mtb to exert cidal activity against non-replicating bacteria under nitrosative stress. After oxathiazolones, N,C-capped dipeptides are only the second class of compounds to show a high degree of selectivity for the proteasome of a pathogen over that of its host. Selectivity was achieved in a novel way, by exploiting that the S3 binding pocket is shallow and wide between 2 subunits in Mtb20S, but narrow and deep between 5 and 6 in human c-20S and between 5i and 6 i-20S, as well as that the S1 binding pocket accommodates large aromatic rings in Mtb 20S but not in human c-20S. A further novelty emerged within the class of N,C-capped dipeptides, in that replacement of P1 phenyl with a naphthyl ring resulted in a change of the inhibition modality from rapid equilibrium to a time-dependent mechanism and increased the residence time of the inhibitor in its binding site, an important goal in drug development for non-covalent inhibitors.

Supplementary Material

Refer to Web version on PubMed Central for supplementary material.

Acknowledgments

We thank Xiuju Jiang for BSL3 technical support. Supported by NIH R56AI080618 (CN), 1R21AI101393 (GL), and the Milstein Program in Chemical Biology of Infectious Diseases. The Department of Microbiology and Immunology is supported by the William Randolph Hearst Foundation.

References

1. Baumeister W, Walz J, Zuhl F, Seemuller E. Cell. 1998; 92:367. [PubMed: 9476896]

- 2. Brown MG, Driscoll J, Monaco JJ. Nature. 1991; 353:355. [PubMed: 1922341]
- 3. Glynne R, Powis SH, Beck S, Kelly A, Kerr LA, Trowsdale J. Nature. 1991; 353:357. [PubMed: 1922342]
- 4. Kelly A, Powis SH, Glynne R, Radley E, Beck S, Trowsdale J. Nature. 1991; 353:667. [PubMed: 1922385]
- Kincaid EZ, Che JW, York I, Escobar H, Reyes-Vargas E, Delgado JC, Welsh RM, Karow ML, Murphy AJ, Valenzuela DM, Yancopoulos GD, Rock KL. Nat Immunol. 2012; 13:129. [PubMed: 22197977]
- 6. Lin G, Hu G, Tsu C, Kunes YZ, Li H, Dick L, Parsons T, Li P, Chen Z, Zwickl P, Weich N, Nathan C. Mol Microbiol. 2006; 59:1405. [PubMed: 16468985]
- 7. Darwin KH, Ehrt S, Gutierrez-Ramos JC, Weich N, Nathan CF. Science. 2003; 302:1963. [PubMed: 14671303]
- 8. Gandotra S, Lebron MB, Ehrt S. PLoS Pathogens. 2010; 6:e1001040. [PubMed: 20711362]
- 9. Gandotra S, Schnappinger D, Monteleone M, Hillen W, Ehrt S. Nat Med. 2007; 13:1515. [PubMed: 18059281]
- 10. Nathan C, Gold B, Lin G, Stegman M, de Carvalho LP, Vandal O, Venugopal A, Bryk R. Tuberculosis (Edinb). 2008; 88(Suppl 1):S25. [PubMed: 18762150]
- 11. Lin G, Tsu C, Dick L, Zhou XK, Nathan C. J Bio Chem. 2008; 283:34423. [PubMed: 18829465]
- 12. Lin G, Li D, de Carvalho LP, Deng H, Tao H, Vogt G, Wu K, Schneider J, Chidawanyika T, Warren JD, Li H, Nathan C. Nature. 2009; 461:621. [PubMed: 19759536]
- 13. MacMicking JD, North RJ, LaCourse R, Mudgett JS, Shah SK, Nathan CF. Proc Nat Acad Sci USA. 1997; 94:5243. [PubMed: 9144222]
- 14. Nathan C. Science. 2006; 312:1874. [PubMed: 16809512]
- 15. Kruger E, Kloetzel PM. Curr Opin Immunol. 2012; 24:77. [PubMed: 22296715]
- 16. Huber EM, Basler M, Schwab R, Heinemeyer W, Kirk CJ, Groettrup M, Groll M. Cell. 2012; 148:727. [PubMed: 22341445]
- 17. Blackburn C, Gigstad KM, Hales P, Garcia K, Jones M, Bruzzese FJ, Barrett C, Liu JX, Soucy TA, Sappal DS, Bump N, Olhava EJ, Fleming P, Dick LR, Tsu C, Sintchak MD, Blank JL. Biochem J. 2010; 430:461. [PubMed: 20632995]
- 18. Bryk R, Gold B, Venugopal A, Singh J, Samy R, Pupek K, Cao H, Popescu C, Gurney M, Hotha S, Cherian J, Rhee K, Ly L, Converse PJ, Ehrt S, Vandal O, Jiang X, Schneider J, Lin G, Nathan C. Cell Host Microbe. 2008; 3:137. [PubMed: 18329613]

$$\begin{array}{c|c}
S2 \\
\hline
N-Cap \\
O \\
R_2 \\
S3
\end{array}$$

$$\begin{array}{c|c}
R_1 \\
N \\
N \\
C-Cap \\
S1
\end{array}$$

Figure 1. Illustration of N,C-capped dipeptides and corresponding binding subsites and structures of DPLG-2 and DPLG-4.

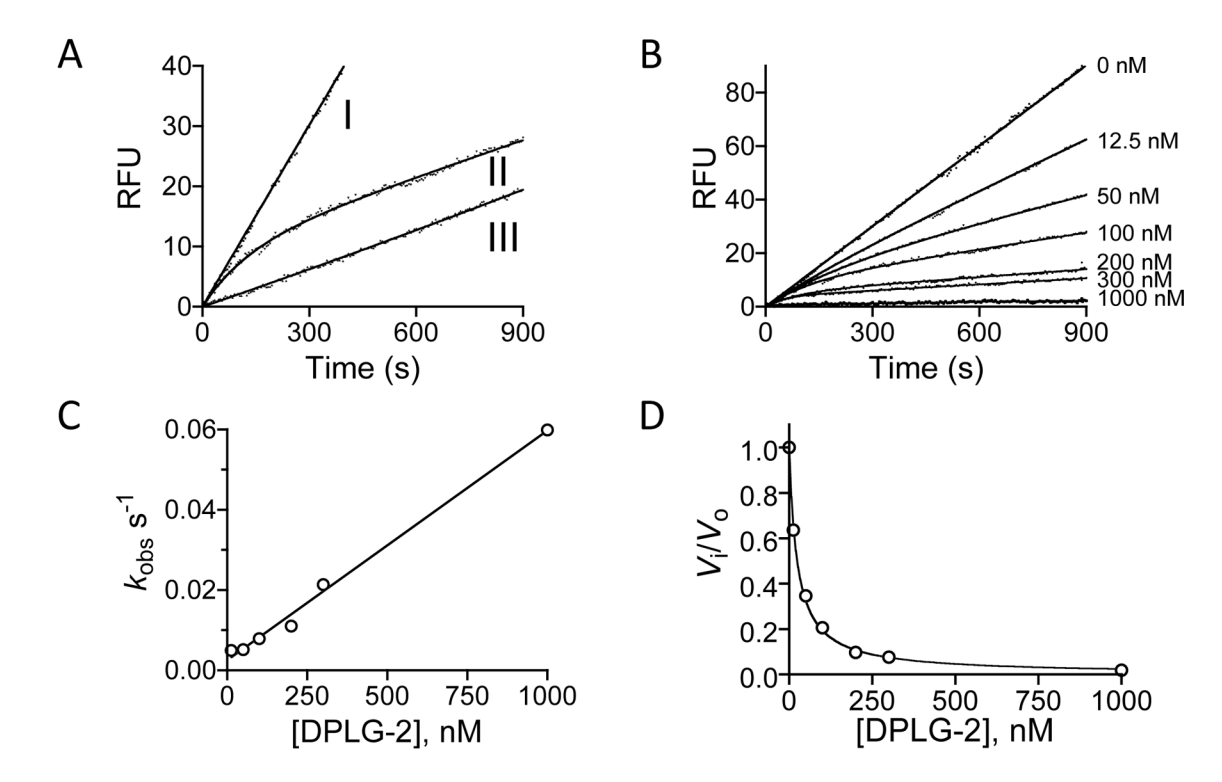


Figure 2. DPLG-2 is a time-dependent inhibitor of the Mtb20S. (A) The proteolytic activity of Mtb20SOG (0.28 nM) with substrate suc-LLVY-AMC (50 \$M) (curve I) following the addition of DPLG-2 (curve II) or ML9 (curve III) at 100 nM. (B) Progress curve of hydrolysis of suc-LLVY-AMC by Mtb20SOG in the presence of DPLG-2. (C) Plot of $k_{\rm obs}$ to DPLG-2 concentrations. (D) Plot of $V_{\rm i}/V_0$ vs inhibitor concentrations.

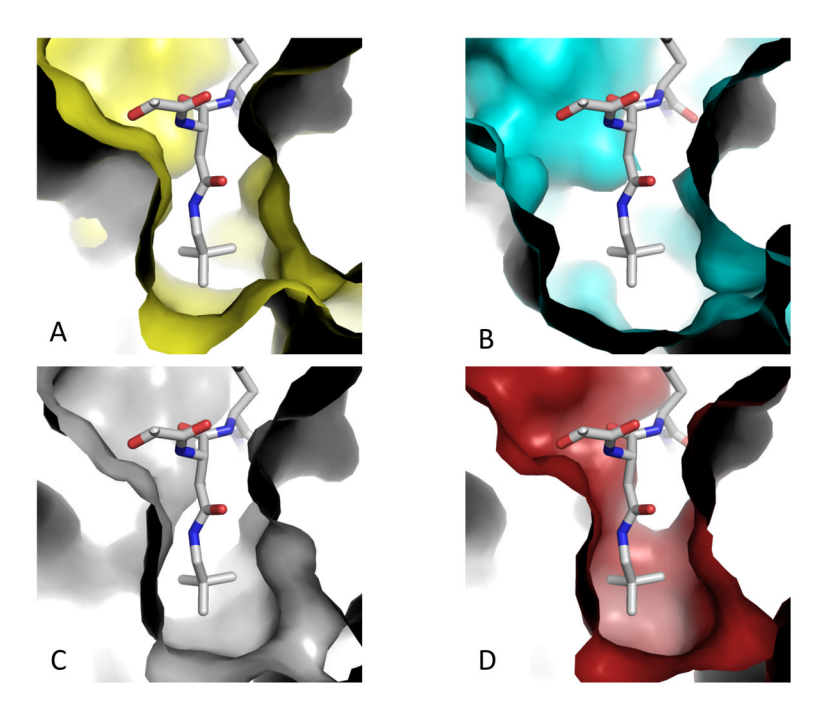


Figure 3. Comparison of the S3 binding pockets between yeast c-20S, Mtb20S, mouse c-20S, and mouse i-20S. The solved co-crystal structure of yeast 20S and ML16 (3MG8) is shown in A), while Mtb20S (2FHG) in B), mouse c-20S (3UNB) in C), mouse i-20S (3UNF) in D) were superimpositions on the solved structure. Figures were made using MacPyMOL (DeLano Scientific, Palo Alto, CA).

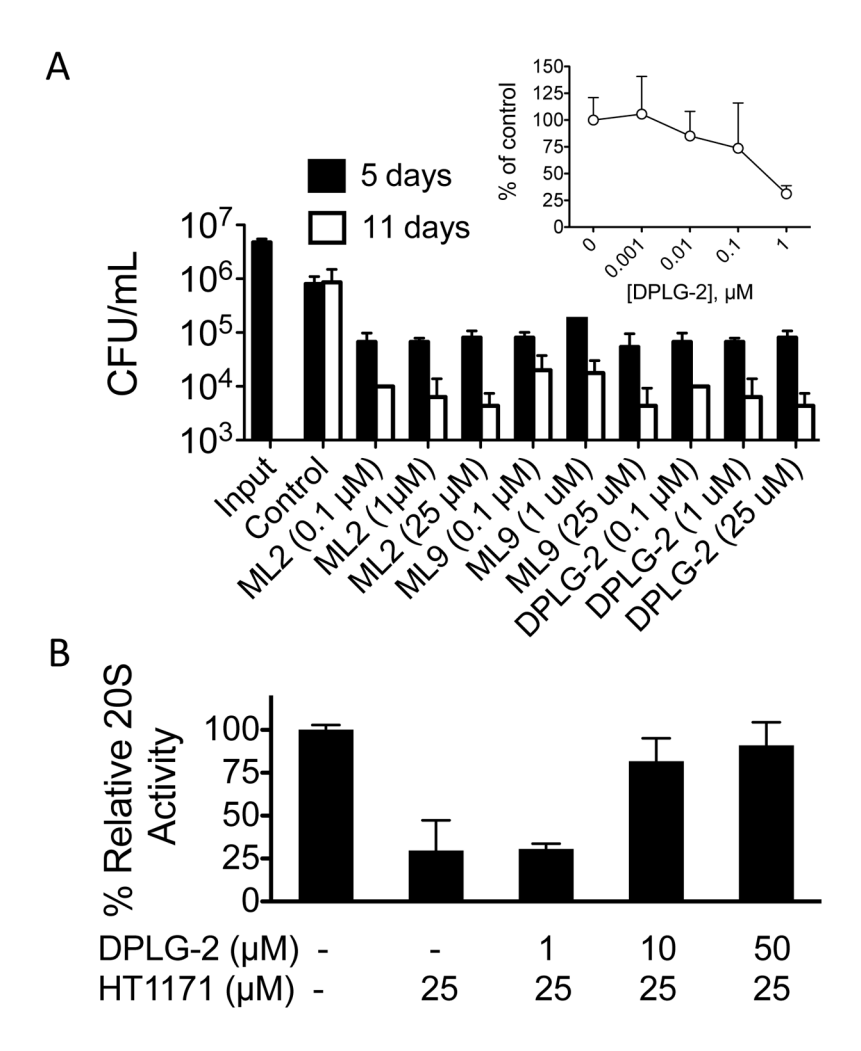


Figure 4.N,C-dipeptides inhibit mycobacterial proteasomes and kill non-replicating Mtb. A) Killing of Mtb H37Rv in Sauton's medium with 0.5 mM NaNO₂ at pH 5.5, which mimics the nitroxidative stress that limits the replication of Mtb in mice. ¹³ Data are means of triplicates in one of at least three experiments. Inset: DPLG-2 kills Mtb in the presence of NaNO₂ at pH 5.5 in a dose-dependent manner. B) BCG cells were incubated with DPLG-2 at indicated concentrations for 4 hours prior to addition of HT1171 and incubated for an additional hour. Proteasome activity in lysates was tested with suc-LLVY-AMC as substrate. Data are means of triplicates of three experiments.

Lin et al.

Table 1

Kis and species-selectivity of N,C-capped dipeptides against Mtb20SOG and human constitutive 20S.

$rac{K_{i(eta 5c)}}{K_{i(Mtb)}}$		77	121	79	0.1	256	16	88
		0.028	0.030	0.038	0.041	0.042	0.042	0.057
K_i (μ М) - 5c (Ac-WLA-AMC) K_i (μ М) - Mtb (Suc-LLVY-AMC)		2.14	3.63	3.00	0.003	10.74	0.67	5.01
<u> </u>	R3	$\mathrm{PhCH}_2\mathrm{CH}_2$	$PhCH_2CH_2$	PhCH ₂ CH ₂	O NH	$PhCH_2CH_2$	$\mathrm{PhCH}_2\mathrm{CH}_2$	N- N
ZI O	R2	N-Et-N-iPr	⟨ ^z ⟩	z o	Neo-pentylamino	z o	N- ^j Pr-N-Pr	N-Et-N-iPr
TZ C	R1	p-F-Phe	p-F-Phe	p-F-Phe	p-F-Phe	н	p-F-Phe	н
R.	ID	ML1	ML2	ML3	ML4	ML5	ML6	ML7

Page 10

Lin et al. 0.05 701 6.8 415 R_i (μ M) - 5c (Ac-WLA-AMC) R_i (μ M) - Mtb (Suc-LLVY-AMC) 0.058 0.068 0.063 0.063 0.070 0.071 29.43 0.003 0.47 8.40 $PhCH_2CH_2$ PhCH₂CH₂ PhCH₂CH₂ PhCH₂CH₂ PhCO B Neo-pentylamino N,N-diethyl NH-'Bu **R**2 p-F-Phe R Ξ ΙŹ ML10 ML12 ML8ML13 ML9А

Page 11

Lin et al.

Table 2

Selectivity of ML2, ML9 and DPLG-2 for Mtb over human c-20S 5c and i-20S 5i

	Ki	K _i µM		V	V
А	Mtb20SOG	5c	5:	$\frac{\Lambda_{i(\beta 5c)}}{K_{i(Mtb)}}$	$\frac{\Lambda_{i(\beta 5i)}}{K_{i(Mtb)}}$
ML2	0:030	3.63	0.82	121	27
ML9	0.063	> 100	26.3	> 1590	417
DPLG-2	0.015	70	54.7	4670	3650

Page 12